RSC Advances

PAPER

View Article Online
View Journal | View Issue

Cite this: *RSC Adv.*, 2017, **7**, 27960

Corannulene–fullerene C_{70} noncovalent interactions and their effect on the behavior of charge transport and optical property†

Yan-Zhi Liu,[a] Kun Yuan, *[ab] Zhao Yuan, [c] Yuan-Cheng Zhu,[a] Sheng-Dun Zhao*[b] and Ling-Ling Lv[a]

Due to the special geometry structures of C_{70} (an ellipsoidal shape with the highest aspect ratio (1 : 1.12) among fullerenes family) and bowl-shaped aromatic hydrocarbons, there are great opportunities for the theoretical computation to deeply explore the "ellipsoid-in-bowl" supra-molecule and their effect on the behavior of charge transport and optical properties. In this study, a new molecular system comprising the non-covalently functionalized complexes of fullerene C_{70} with corannulene is investigated *via* the dispersion-corrected density functional theory calculations. Based on the interaction modes, two and three different kinds of configurations have been located on the potential surfaces of the 1 : 1 and 2 : 1 corannulene@C_{70} complexes, respectively. A comprehensive study of binding energy, ionization energy, electron affinity, intermolecular weak interaction regions, the frontier molecular orbitals and gaps, and absorption spectra unravels the structure–property relationship of the complexes. By using the charge hopping rate based on Marcus theory, the charge transport properties of the complexes were discussed. The results shows that the electron transport was more efficient and fast than the hole when C_{70} interacts with two corannulene molecules by its polar positions. In additional, the modification of C_{70} on its equatorial position with two corannulene is better for acquiring relative high charge mobility than on polar position with one or two. The electronic transitions and UV-vis absorption spectra of the complexes are mainly determined by the constituent molecule of C_{70} but hardly dependent on corannulene moiety. Meanwhile, it is found that the more numbers of corannulene noncovalently bonded, the more red-shifted of electron absorption of C_{70} is.

Received 6th April 2017
Accepted 17th May 2017

DOI: 10.1039/c7ra03923a

rsc.li/rsc-advances

1. Introduction

Noncovalent functionalization of sp^2 carbon materials has received tremendous interest since it offers the possibility of attaching a functionality while maintaining the integrity of the sp^2-hybridized carbon network, that is, without disturbing the electronic properties of the substrate.[1] The non-covalently functionalized complexes of carbon nanomaterials are among the various derivatives which find a myriad of applications in organic electronics,[2,3] light-harvesting[4] and organic field-effect transistors.[5] On the other hand, a supramolecular combination of carbon nano-materials, such as single-wall carbon nanotubes and fullerenes,[6–8] nano-ring and fullerene,[9–12] constitutes a unique class of molecular assemblies and devices. The structure of this complex is composed of curved π-systems with a concave–convex interface, and its assembly is driven essentially by van der Waals interactions.[13,14]

Although sp^2 carbon materials have extraordinary mechanical and electronic proprieties, one of the main drawbacks of these materials is their poor solubility in the common solvents or matrix used in the applications. In recent years, supramolecular approaches[15–17] have been employed to overcome this problem even to improve their performances. Based on noncovalent interactions, pyrene derivatives are used as a dispersing agent for favoring nanotube dispersion in different solvents.[18] Moreover, Joshi and Ramachandran[19] have studied the noncovalent interactions in the complexes of indigo wrapped over carbon nanotubes (CNT) by means of the dispersion corrected density functional theory method. It was found that indigo forms stable noncovalent complexes with carbon nanotubes. These complexes showed distinct electronic properties compared to the component species. Unlike bare CNT and indigo, the complexes absorb in a broad range in the visible region, making them suitable for solar cell applications; the

[a]College of Chemical Engineering and Technology, Tianshui Normal University, Tianshui 741001, China. E-mail: tsnuyk@yeah.net
[b]Institute for Chemical Physics, Department of Chemistry, School of Science, State Key Laboratory of Electrical Insulation and Power Equipment, School of Mechanical Engineering, Xi'an Jiaotong University, Xi'an 710049, China. E-mail: sdzhao@mail.xjtu.edu.cn
[c]Department of Chemical and Biomedical Engineering, Florida State University, Tallahassee, 32306, USA

† Electronic supplementary information (ESI) available. See DOI: 10.1039/c7ra03923a

charge transport properties of a complex can be tuned by changing the orientation of the adsorbed molecule.

Particularly, it is important to prevent the aggregation of unfunctionalized fullerene in photovoltaic blends for replacing the commonly employed butyric acid methyl ester derivatives functionalized fullerene with economical and light harvesting advantages and performances. Recently, Cominetti *et al.*[20] have demonstrated that the use of a pyrene derivative (1-pyrenebutyric acid butyl ester, PyBB) is effective in preventing the aggregation of fullerene in photovoltaic blends made of regioregular poly(3-hexylthiophene). In additional, as indicated by the photo-induced electron transfer in C_{60}-pyrene films[21] or by the energy transfer in pyrene appended C_{60} and C_{70} derivatives,[22] the π–π interaction between pyrene and fullerene molecules can promote the dispersion of the acceptor in the polymer matrix at the molecular level and favors electronic processes. Very recently, Carati, *et al.*[23] have explored the interactions between PyBB and unfunctionalized C_{60} or C_{70} blended with poly({4,8-bis[(2-ethylhexyl)oxy]benzo[1,2-*b*:4,5-*b*′] dithiophene-2,6-diyl}{3-fluoro-2-[(2-ethylhexyl)carbonyl]thieno [3,4-*b*]thiophenediyl}) as electron donor. Both the spectroscopic and the electrical investigation indicated that PyBB addition has important consequences on the morphology of the blends as well as on their charge transport properties.

Supramolecular order determines to a large extent the performance of these carbon nanostructures within a device. It is known that corannulene belongs to a typical curved carbon π-systems, and fullerene C_{70} has an ellipsoidal shape with long (0.796 nm) and short axes (0.712 nm) and has the highest aspect ratio (1 : 1.12) among fullerenes family.[24] Therefore, stable complexes could be formed by host–guest interactions between C_{70} and corannulene. Concurrently, corannulene is a typical bucky bowl carbon-rich organic molecule, which is the smallest nonplanar fullerene fragment ($C_{20}H_{10}$). Inherently, it has well geometric matching with fullerenes. Therefore, the interaction between fullerenes C_{70} and corannulene with an anisotropic shape is of great interest because, unlike for spheroidal C_{60}, several geometrically distinct orientations are possible. By means of density functional theory (DFT) protocols, Casella and Saielli[25] presented a theoretical investigation of the complexation thermodynamics of complexes of C_{70} and C_{60} fullerenes with bowl-shaped hexabenzocoronene derivatives. For C_{70} they have considered two different orientations with respect to the bowl surface: either with the long axis of C_{70} parallel to the bowl or perpendicular to it. In recent, a class of outstanding fullerene receptors was developed by Denis and his co-worker.[26] They designed and studied new fullerene receptors which are constructed employing porphyrins, single or multi-corannulene pincers and metallic centers. Theoretical calculations indicated that if porphyrin and corannulene pincers are merged, the strongest hosts for fullerenes can be built.

Recently, Josa *et al.* have carried out several comprehensive studies for the stacking interactions between corannulene or sumanene (including their derivatives) with different sizes and fullerene, for both C_{60} and C_{70} by using dispersion-corrected DFT.[27–29] No doubt, these works would be very essential for providing considerable improvement in the task of fullerene recognition, or helpful for finally finding the best buckybowl to improve the efficiency and/or selectivity of future buckycatchers for fullerene. Although the interaction behaviors between fullerenes and corannulene or sumanene have been deeply studied, their supramolecular spectral and electronic properties are seldom explored. Moreover, the filling of the interior space of the corannulene with nanoscale materials results in novel nano-hybrid with interesting properties and unique functions including electron and optical characters, which may be very different from the individual components. In this work, we theoretically investigate the structures and properties of 1 : 1 and 2 : 1 supramolecular complexes formed with corannulene and C_{70}. Especially, the behaviors of charge transport and optical properties of the corannulene@C_{70} supramolecular systems at a molecular level by quantum chemical method are discussed. We hope that the present study would be helpful for the deep understanding to the experimental results of π–π noncovalent wrapped fullerene-based electric device and materials.

2. Computational methods

In the current work, the density functional theory of Grimme's DFT-D3 (ref. 30) was mainly employed for the study of corannulene@C_{70} systems. DFT-D3 method provides an empirical dispersion correction for DFT.[30,31] The ability of this new density functional to predict and explain the supramolecular chemistry at van der Waals distances is very encouraging since density functional theory can be used conveniently for supramolecular systems.[32,33] All the geometric configurations were fully optimized at the B3LYP-D3/6-31G(D) levels. No symmetry constraints were applied during optimizations. Harmonic frequency analyses were performed at the same level to confirm that these structures were local minima or transition state on the potential energy surfaces. The intermolecular interaction energies (ΔE_{int}^{cp}) with basis set superposition errors (BSSE) corrected were calculated by the counterpoise method.[34] The ionization energy and the electron affinity of the complexes were calculated from the energies of the optimized geometries of corresponding charged and neutral systems. The transport of charge carriers at room temperature was studied using the hopping model based on Marcus theory.[35,36] The transfer integral (t) and the internal reorganization energy (λ) of the carriers were computed to assess the rate constant of charge transfer (k_{CT}).[36] The foregoing parameters along with the diffusion coefficient (D) and the charge carrier mobility (μ) were determined using the equations given in ref. 36. The excited state calculations were done using the TD-DFT by the same method and basis set. Additionally, a visual study of intermolecular noncovalent interaction between host and guest was performed *via* calculating the reduced density gradient (RDG),[37] coming from the electron density ($\rho(r)$) and its first derivative ($RDG(r) = 1/(2(3\pi^2)^{1/3})|\nabla\rho(r)|/\rho(r)^{4/3}$), and the second largest eigenvalue of Hessian matrix of electron density (λ_2) functions by using Multiwfn program.[38,39] All the other calculations were performed with the Gaussian 09 program.[40]

3. Results and discussion

Geometric configurations

Bowl-shaped aromatic hydrocarbons exemplify well Euler's rule concerning the insertion of five-membered rings in a hexagonal net to induce curvature.[41] Corannulene, $C_{20}H_{10}$, with one central five-membered ring, is the parent structure to which other bowls are often compared.[42] As having been mentioned, the encapsulation of fullerenes C_{70} by corannulene with an anisotropic shape is of great interest because, unlike for spheroidal C_{60}, two geometrically distinct orientations are possible. All the geometric configurations of the 1 : 1 and 2 : 1 corannulene@C_{70} complexes obtained at B3LYP-D3/6-31G(D) level are shown in Fig. 1. In addition, the Cartesian coordinates of optimized complexes included in this work are available in the ESI.†. As expectedly, two and three different kinds of configurations can be located on the potential surfaces of the 1 : 1 and 2 : 1 corannulene@C_{70} complexes, respectively. In order to ensure that these complexes are global minimums, we made a 36° rotation of C_{70} around its long axis for the complexes be re-optimized (36° rotation was selected because the C_{70} belongs to D_{5h} point group. It can be imagined that when C_{70} rotates by 72° around its long axis in the cave of corannulene, an equivalent complex would be obtained, but when it rotates by 36°, a conformational isomer complex may be obtained). However, it is found that the new initial structures all automatically returned to the pre-rotated configurations. Namely, the new obtained complex is nearly with the same geometry parameters and energy to the originally optimized structure, indicating that the obtained complexes are global minimums. For ease of discussion, these different configurations are denoted as *n*Cor@C_{70}-S, -L and -SL ($n = 1$ or 2), which correspond to C_{70}-standing and -lying orientations in the cavities of corannulene, respectively.

As shown in Fig. 1, the interfacial distances (d_i) between corannulene and C_{70} of the complexes, which is an important parameter for the charge transport calculations and will be discussed later, is defined as lengths between the centroids (red dots in Fig. 1) of the pentagon unit of corannulene and the nearest centroid of a hexagon or pentagon of C_{70}. It is known that the interplanar π–π van der Waals interaction distance between graphite sheets is 3.4 Å. In fact, 3.4 Å is regard as a benchmark and the most nice π–π van der Waals interaction distance either in planar–planar or in convex–concave π–π systems.[32,43,44] Generally, if the distance between host and guest is smaller than 3.4 Å, the repulsion would be increase. In the C_{70}-standing configurations, d_i are found to be within the ranges of 3.54–3.55 Å; those in C_{70}-lying configurations are within the ranges of 3.66–3.67 Å, which are very close to the equilibrium distances defined by Josa *et al.* using the self-consistent charge density functional tight-binding method together with an empirical correction for the dispersion (SCC-DFTB-D).[27] Meanwhile, those interfacial distances are not significantly far away from the 3.4 Å, a van der Waals distance between graphite sheets, thereby accounting for strong π–π interactions and well mutual-fitting between corannulene and C_{70} either in case of C_{70}-standing or C_{70}-lying orientation.

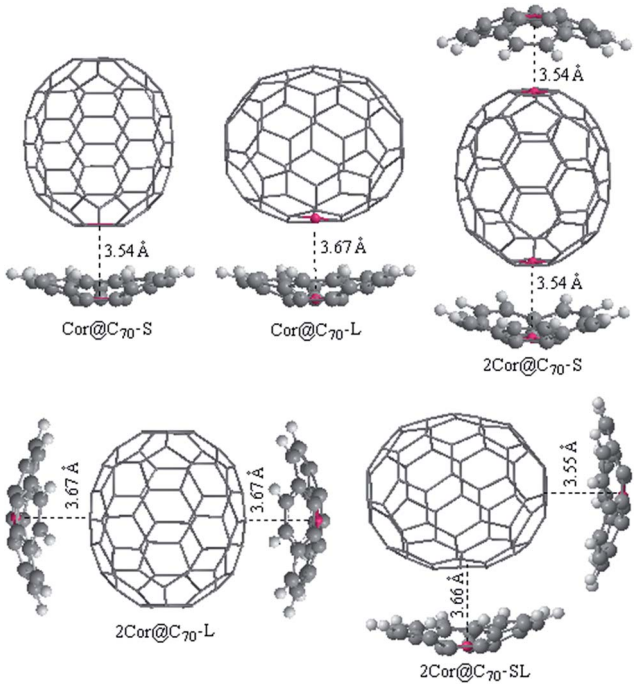

Fig. 1 The optimized geometries of Cor@C_{70}-S, Cor@C_{70}-L, 2Cor@C_{70}-S, 2Cor@C_{70}-L and 2Cor@C_{70}-SL.

Interaction energies and thermodynamic properties

Binding energy is very valuable and necessary for measuring the stability and strength of intermolecular noncovalent interaction of Cor@C_{70} systems. In Table 1, with and without BSSE corrected binding energies (ΔE_{CP} and ΔE) are tabulated. For the Cor@C_{70}-L complex, the ΔE_{CP} is about 17.11 kcal mol^{-1}, which is close to the previous works of other groups computing at B97-D2/TZVP level.[27–29] It is noted that the ΔE_{CP} of Cor@C_{70}-L is slightly larger than that in Cor@C_{70}-S by 1.53 kcal mol^{-1}, indicating that the stability of Cor@C_{70}-L is stronger than that of Cor@C_{70}-S, namely C_{70} is preferred to adopt the lying orientation in the cavity of corannulene. In additional, it is noted that, for the same C_{70} orientation, the ΔE_{CP} in 2 : 1 complexes are close to twice as much as those of 1 : 1 complexes, suggesting an additive nature of binding energy

Table 1 With and without BSSE (kcal mol^{-1}) corrected binding energy (ΔE_{CP} and ΔE, kcal mol^{-1}) between corannulene and C_{70}, the changes of Gibbs free energy (ΔG, kJ mol^{-1}), enthalpy (ΔH, kJ mol^{-1}) and entropy (ΔS, J mol^{-1} K^{-1}) of the formations of the five different complexes

Complexes	ΔE	BSSE	ΔE_{CP}	ΔG	ΔH	ΔS
Cor@C_{70}-S	−21.09	5.51	−15.58	−22.94	−86.11	−50.64
Cor@C_{70}-L	−23.05	5.94	−17.11	−34.02	−92.22	−46.65
2Cor@C_{70}-S	−42.11	11.00	−31.11	−5.32	−124.18	−95.28
2Cor@C_{70}-L	−45.97	11.79	−34.18	−14.59	−135.48	−96.91
2Cor@C_{70}-SL	−45.39	11.69	−33.70	−18.89	−131.75	−90.47

against number of the involved molecules. Obviously, the stabilization of the complexes is derived from the concave–convex π–π interactions.[45]

The thermodynamic information of the encapsulations of C_{70} by the corannulene at 298.15 K and 1 atm obtained by using (DFT) calculations at the B3LYP-D3/6-31G(D) level of theory are also given in Table 1. It can be seen that the relative order of the ΔG and ΔH of the 1 : 1 complexes are all well consistent with those of the ΔE_{CP}. The binding process of C_{70} by corannulene in the vacuum are exergonic and spontaneous, with ΔG values −22.94 and −34.02 kJ mol^{-1} for Cor@C_{70}-S and Cor@C_{70}-L, respectively. For two 1 : 1 complexes, ΔG of Cor@C_{70}-L is larger (more negative) than that of Cor@C_{70}-S, manifesting the spontaneous trend of formation of C_{70}-lying configuration is stronger than that of C_{70}-standing configuration. Moreover, it is worthy to note that the ΔG of 2 : 1 complexes are obviously smaller than those of two 1 : 1 complexes, meaning that the thermodynamic spontaneous trend of C_{70} binding the second corannulene molecule is weaker than that of C_{70} binding the first one. Especially, the ΔG of 2Cor@C_{70}-S is only −5.32 kJ mol^{-1}, suggesting that it is not easy to binding two corannulene molecules at the regions of two polar positions of C_{70}. Because of the number of the free molecules decreasing by a half or two-thirds after the formations of the 1 : 1 or 2 : 1 complexes, the entropies of the present five complexes decrease by 47–97 J mol^{-1} K^{-1}. According to the ΔH values, all the Cor@C_{70} binding reactions are found to be exothermic. All these thermodynamic information indicate that the binding of C_{70} by corannulene in the vacuum is enthalpy-driven and entropy-opposed, which is utterly same to the carbon nanoring@fulleren systems.[9,10]

Weak interaction regions and frontier orbital features

Intermolecular weak interactions can be detected and visualized in real space based on the electron density ρ and its derivatives,[37] *viz.* the reduced density gradient (RDG), coming from the electron density ($\rho(r)$) and its first derivative ($RDG(r) = 1/(2(3\pi^2)^{1/3})|\nabla\rho(r)|/\rho(r)^{4/3}$), and the second largest eigenvalue (λ_2) of Hessian matrix of electron density functions. Fig. 2 shows the visualized weak interaction regions of the Cor@C_{70}-S and Cor@C_{70}-L complexes and their corresponding scatter graphs. The dish-shaped region marked with green accompanied with light-brown around C_{70} can be identified as weak interaction region (Fig. 2, left) between the corannulene and C_{70}. In these regions, it mirrors concave–convex π–π van der Waals interaction. The spike marked with green circle (Fig. 2, right) is correlating with π–π van der Waals interaction of the host and guest, and the electron density around this spike is low to zero.

It is noted that the edge of the weak interaction regions between corannulene and C_{70} present wavelike-shapes (Fig. 2, left), this is derived from the characteristic of corannulene molecular structure with five-membered rings in a hexagonal net. Additionally, qualitatively seen from Fig. 2 (a and b, left), the π–π van der Waals interaction area in Cor@C_{70}-L is larger than that in Cor@C_{70}-S, which is well consistent with the relative order of the binding energies.

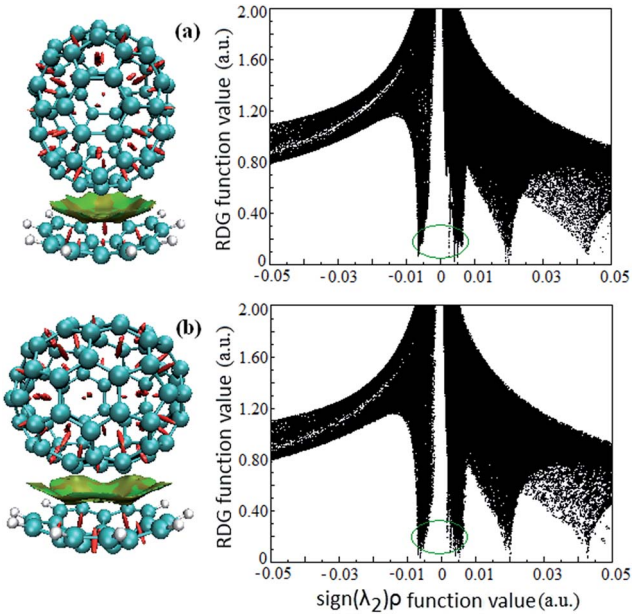

Fig. 2 The visualized weak interaction regions (left) and the scatter graph (right) of the (a) Cor@C_{70}-S and (b) Cor@C_{70}-L complexes.

It is known that molecular orbital are not physical observables. However, the properties of the frontier orbital are often closely related to the photo-electron behaviors and spectrum properties. Fig. 3 presents the compositions and energy levels of the highest occupied molecular orbital (HOMO) and the lowest unoccupied molecular orbital (LUMO) of C_{70} and the five different complexes. As Fig. 3 showing, the energies of the HOMOs and LUMOs of the five complexes are close to those of the free C_{70}. Consequently, the compositions of HOMOs and LUMOs of the complexes completely derive from the HOMO and LUMO of C_{70}, respectively. The frontier molecular orbital of the complexes are completely localized on the C_{70} but independent of the moiety of corannulene, indicating the lack of charge transfer between the corannulene and C_{70} during the formations of the complexes,[46] which is different from indigo@carbon-nanotubes systems.[19] Significantly, what above suggests that the lowest-energetic electron transition (HOMO → LUMO) of the complexes would take place in the intramolecule of C_{70} rather than between the corannulene and C_{70} molecule, that is no photoinduced charge transfer phenomenon occurring during photoexcitation.

The HOMO–LUMO energy gaps of the complexes are close to that of C_{70} but much smaller than that of corannulene (listed in Table 2). Meaningfully, compared to that of free C_{70}, the $gap_{HOMO-LUMO}$ of Cor@C_{70}-S and 2Cor@C_{70}-S are slightly increased by 0.01–0.02 eV, while those of other three complexes are slightly decreased by 0.02–0.04 eV. Therefore, the introducing an additional molecule of corannulene onto the C_{70} at different position does not change the energy gap significantly predicting that the electronic transition properties of the C_{70} would be less affected upon further addition of corannulene.

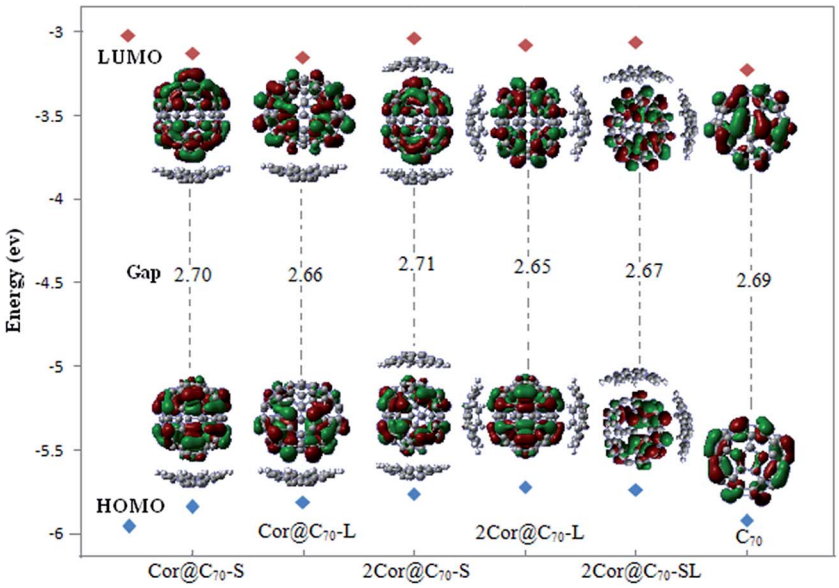

Fig. 3 The frontier molecular orbital and the corresponding energy level diagram of the C_{70} and five complexes.

Table 2 The vertical ionization energy (IPv, eV), adiabatic ionization energy (IPa, eV), vertical electron affinity (EAv, eV), adiabatic electron affinity (EAa, eV) and the HOMO–LUMO energy gap (eV) for corannulene, C_{70} and their complexes

Systems	IPv	IPa	EAv	EAa	$Gap_{HOMO-LUMO}$
Corannulene	7.49	7.38	−0.04	−0.17	4.39
C_{70}	7.10	7.02	−2.07	−2.14	2.69
Cor@C_{70}-S	6.92	6.83	−2.02	−2.11	2.70
Cor@C_{70}-L	6.87	6.76	−2.03	−2.12	2.66
2Cor@C_{70}-S	6.86	6.69	−2.05	−2.06	2.71
2Cor@C_{70}-L	6.73	6.62	−2.00	−2.10	2.65
2Cor@C_{70}-SL	6.76	6.65	−1.98	−2.08	2.67

Electronic properties and behavior of charge transport

Electronic behaviors and properties of the complexes can be obtained by investigating the molecular ionization potential and electron affinity which can be calculated by removing or adding an electron from the monomers or supramolecular complexes (the Cartesian coordinates of those optimized anion and cation complexes are available in the ESI†). Table 2 lists the computed values of vertical ionization energy (IPv), adiabatic ionization energy (IPa), vertical electron affinity (EAv) and adiabatic electron affinity (EAa) of corannulene, C_{70} and their complexes. It is found that either the vertical ionization energy or adiabatic ionization energy of free corannulene is larger than those of free C_{70}, indicating that either the electron-denoting or electron-accepting of C_{70} is stronger than corannulene in their isolated state. Thereby, $gap_{HOMO-LUMO}$ of corannulene is distinctly larger than that of C_{70}. As having been noted, the frontier molecular orbital of the five complexes are completely derived from those of C_{70} but independent of corannulene. Either ionization energies or electron affinities of the complexes should be mainly determined by moiety of C_{70}. In fact, as listed in Table 2, both the ionization energies and electron affinities of the complexes are all close to those of C_{70}, while they are all smaller than those of free C_{70}.

In additional, the ionization energies of C_{70}-lying configurations are smaller than those of C_{70}-standing ones, while the electron affinities of C_{70}-lying configurations are similar to those of C_{70}-standing ones. Therefore, comparing to by polar position, noncovalent functionalization of C_{70} with corannulene by its equatorial position is more favorable to increase the capability of electron-denoting but less affects that of electron-accepting. Furthermore, ionization energies of the three 2 : 1 complexes are smaller than those of the two 1 : 1 complexes; meanwhile, electron affinities of them are slightly smaller than those of two 1 : 1 complexes, meaning that the capability of electron-denoting of C_{70} would be enhanced but capability electron-accepting would be weakened with the number of wrapped corannulene increasing from one to two. By contrast, the relatively low value of ionization energy and electron affinity for the complexes with respect to introducing the noncovalent binding of corannulene would favor to the creation of holes but against to injection of electrons for fullerene C_{70}.

Charge mobility calculations were performed to obtain more insight into the charge transport properties of these supramolecular systems. The carrier mobility depends on various parameters including the transfer integral, reorganization energy, rate constant for charge carrier transport and the distance between the molecules. The calculated values of these parameters are listed in Table 3, where + and − signs represent the hole and the electron, respectively. The high value of the transfer integral for the hole transport can be correlated with the high values of the rate constant and the diffusion coefficient which in turn increases the hole mobility.[19] Because the reorganization energies of electrons ($\lambda_+ = 0.174$ eV) and holes ($\lambda_- = 0.177$ eV) are nearly the same in 2Cor@C_{70}-SL, the transfer rate

Table 3 The calculated value of transfer integral (t, eV), internal reorganization energy (λ, eV), rate constant (k_{CT}, s^{-1}), diffusion coefficient (D, cm^2 s^{-1}) and carrier mobility (μ, cm^2 V^{-1} s^{-1})

Systems	Distance/Å	t_+	t_-	λ_+	λ_-	k_{CT^+}	k_{CT^-}	D_+	D_-	μ_+	μ_-
Cor@C_{70}-S	3.54	3.0×10^{-4}	8.0×10^{-5}	0.142	0.16	1.01×10^{9}	5.67×10^{7}	6.3×10^{-7}	3.6×10^{-8}	2.43×10^{-5}	1.38×10^{-6}
Cor@C_{70}-L	3.67	3.0×10^{-3}	2.0×10^{-3}	0.171	0.163	3.08×10^{10}	3.41×10^{10}	2.1×10^{-5}	2.3×10^{-5}	8.03×10^{-4}	8.89×10^{-4}
2Cor@C_{70}-S	3.54	4.0×10^{-4}	4.0×10^{-4}	0.212	0.095	7.42×10^{8}	3.46×10^{9}	4.6×10^{-7}	2.2×10^{-6}	1.80×10^{-5}	8.39×10^{-5}
2Cor@C_{70}-L	3.67	4.9×10^{-3}	7.1×10^{-3}	0.166	0.174	1.97×10^{11}	3.73×10^{11}	1.3×10^{-4}	2.5×10^{-4}	5.14×10^{-3}	9.74×10^{-3}
2Cor@C_{70}-SL	3.55	3.7×10^{-3}	1.0×10^{-3}	0.174	0.177	1.01×10^{11}	7.13×10^{9}	6.4×10^{-5}	4.5×10^{-6}	2.48×10^{-3}	1.74×10^{-4}
	3.66							6.8×10^{-5}	4.8×10^{-6}	2.63×10^{-3}	1.85×10^{-4}

and carrier mobility depend mainly on the transfer integral. Most interestingly, t_- in all complexes except for 2Cor@C_{70}-L shows a smaller value than t_+, higher k_- was obtained for 2Cor@C_{70}-L. Therefore, the electron transport was more dominant than the hole transport in Cor@C_{70}-L complex. That is, the electron transport was more efficient and fast than the hole when C_{70} interacts with two corannulene molecules by its polar positions. The distance between the molecules affects the diffusion coefficient and hence the carrier mobility.[36] For the 2Cor@C_{70}-SL, separated by a longer distance of 3.66 Å, the hole and electron mobilities are 2.63×10^{-3} and 1.85×10^{-4} cm^2 V^{-1} s^{-1} higher, respectively.

For 1 : 1 complexes, both the hole and electron mobilities of the Cor@C_{70}-L are one or two order higher than those of the Cor@C_{70}-S. For 2 : 1 complexes, those of the 2Cor@C_{70}-L are nearly two orders higher than those of 2Cor@C_{70}-S, suggesting that the noncovalent binding fullerene C_{70} with corannulene can obviously alter its transport properties. For 2Cor@C_{70}-SL, its charge mobilities are only slightly smaller than those of 2Cor@C_{70}-L but significantly larger than those of 2Cor@C_{70}-S. Therefore, the above results indicate that the modification of C_{70} on its equatorial position (C_5 symmetry axis of corannulene parallel to the long axis of C_{70}) with two corannulene is better for acquiring relative high charge mobility than on polar position with one or two.

Electronic transitions and UV-vis absorption spectra

The UV-vis absorption spectra and the main corresponding transition composition of C_{70} and corannulene molecules and their complexes are determined using the time-dependent

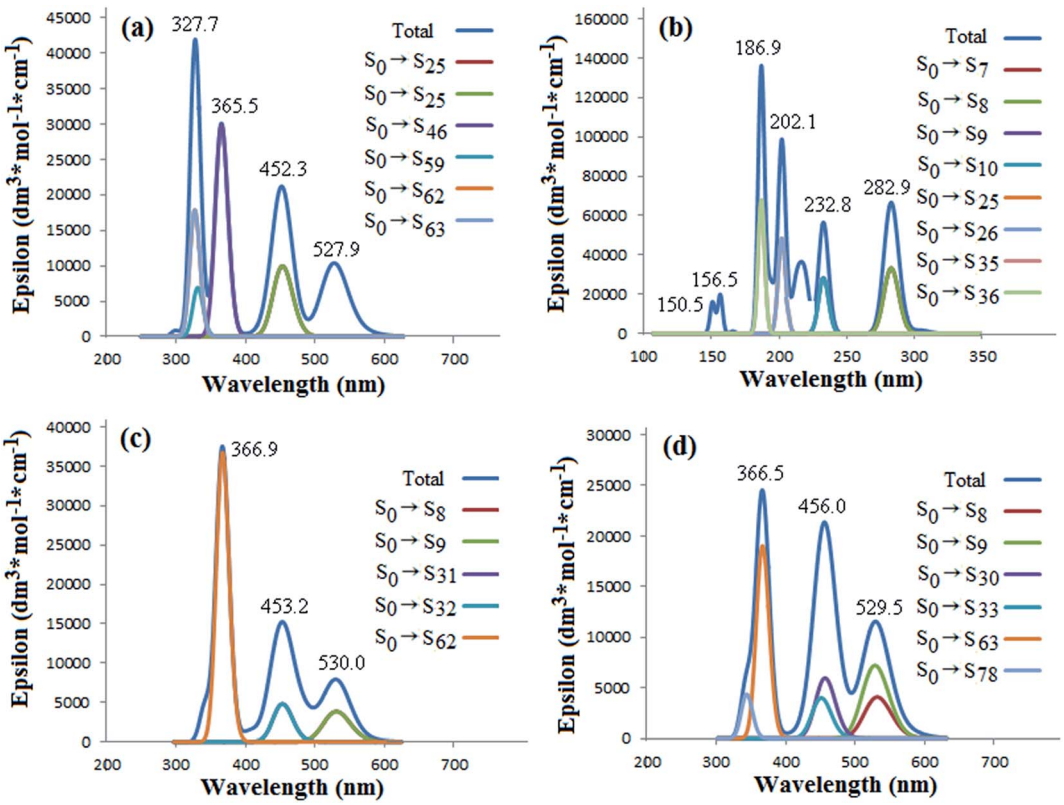

Fig. 4 Simulated UV-vis absorption spectra and the main corresponding transition composition (a) C_{70}, (b) Cor, (c) Cor@C_{70}-S and (d) Cor@C_{70}-L.

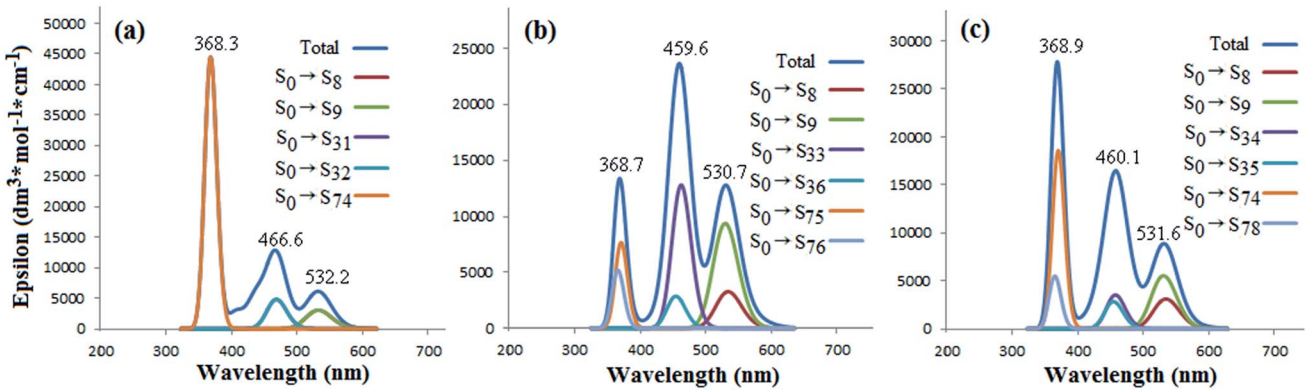

Fig. 5 Simulated UV-vis absorption spectra and the main corresponding transition composition (a) 2Cor@C_{70}-S, (b) 2Cor@C_{70}-L and (c) 2Cor@C_{70}-SL.

density functional theory (TD-DFT) method and depicted in Fig. 4 (free moiety and 1 : 1 complexes) and Fig. 5 (2 : 1 complexes). The characteristic peaks of the free corannulene are substantially different from that of the fullerene C_{70}. It is clear that the absorption peaks of C_{70} appear in the longer range of 300–600 nm (UV-vis region), in which the highlighted peaks have been labeled as 327, 365, 452 and 527 nm, correlating with the contributions of the $\pi \rightarrow \pi^*$ transitions with different energy levels ($S_0 \rightarrow S_n$, Fig. 4(a)), respectively, but those of free corannulene appear in the shorter range of 150–300 nm (UV region) which mirror to the sigma (σ) and π electron transitions. Therefore, the electronic transitions of corannulene are more difficult than C_{70}. This is well coincide to the fact of significant difference of $gap_{HOMO-LUMO}$ between C_{70} and corannulene (Table 2). In additional, corannulene is a kind of chemically inert noncovalent functional reagent of C_{70}. The electronic transitions and UV-vis absorption spectra of the nCor@C_{70}-S, -L and -SL ($n = 1$ or 2) would be mainly determined by the constituent molecule of C_{70} but hardly dependent on corannulene.

As Fig. 4(c) and (d) showing, in the absorption spectra of the Cor@C_{70}-S and Cor@C_{70}-L complexes, the characteristic peaks of corannulene do not appear, and the three prominent peaks of them appear at the positions similar to those of free C_{70} only with no more than 4 nm red-shifts. The largest contributions for the peak at 366 nm of Cor@C_{70}-S and Cor@C_{70}-L derived from transitions of $S_0 \rightarrow S_{62}$ and $S_0 \rightarrow S_{63}$, respectively (Fig. 4(c) and (d)). Although the maximum absorption wave lengths of Cor@C_{70}-S and Cor@C_{70}-L are nearly the same, the corresponding absorption strengths and transition composition are of some difference, which maybe brings by the difference of the electron transition probabilities in different configurations.

For UV-vis absorption spectra of the three 2 : 1 complexes (Fig. 5), three prominent peaks are also presented, respectively. The highlighted peaks have been labeled as 368, 467, and 532 nm for 2Cor@C_{70}-S, also correlating with the contributions of the $\pi \rightarrow \pi^*$ transitions with different energy levels ($S_0 \rightarrow S_n$, Fig. 5(a)). It is noted that wave lengths of the three maximum peaks are all longer than those of 1 : 1 complex of Cor@C_{70}-S; meanwhile, those of 2Cor@C_{70}-L are longer than those of Cor@C_{70}-S. So does for those of 2Cor@C_{70}-SL. What above results suggest the more numbers of corannulene noncovalent-bond, the more red-shifted of electron absorption of C_{70}. Additionally, it is found that the largest contributions for the maximum peaks at 368.3 nm of 2Cor@C_{70}-S and 459.6 nm of 2Cor@C_{70}-L derived from transitions of $S_0 \rightarrow S_{74}$ (Fig. 5(a)) and $S_0 \rightarrow S_{33}$ (Fig. 5(b)), respectively. Interestingly, in the total absorption curve, 2Cor@C_{70}-SL shows a very similar features as 2Cor@C_{70}-S in 300–400 nm region and as 2Cor@C_{70}-L in 400–600 nm region, suggesting that corannulene located on the polar position affects electronic transitions of 2Cor@C_{70}-SL in UV region and that located on the equatorial position affects electronic transitions in visible region.

4. Conclusion

Because of the anisotropic feature of the fullerene C_{70}, the supramolecular complexes formed with bowl-shaped curved aromatic corannulene ($C_{20}H_{10}$) and C_{70} are diversity and interesting. In this paper, the noncovalent interactions in the 1 : 1 and 2 : 1 complexes formed with corannulene and fullerene C_{70} are studied by means of the dispersion corrected density functional theory method (DFT-B3LYP-D3). It was found that C_{70} is preferred to adopt the lying orientation in the cavity of corannulene due to a larger concave–convex π–π interactions area than the standing orientation. The binding energies between corannulene and C_{70} in 2 : 1 complexes are close to twice as much as those of 1 : 1 complexes, suggesting an additive nature of binding energy against number of the involved molecules. The thermodynamic information indicates that the noncovalent wrapping of C_{70} by corannulene in the vacuum is enthalpy-driven and entropy-opposed.

The frontier molecular orbital of the complexes are completely localized on the C_{70} but independent of the moiety of corannulene, indicating the lack of charge transfer between the corannulene and C_{70} during the formations of the complexes. The ionization energies and the electron affinities shows that, comparing to by polar position, noncovalent functionalization of C_{70} with corannulene by its equatorial position is more favorable to increase the capability of electron-denoting

but less affects that of electron-accepting. Moreover, the capability of electron-denoting of C_{70} would be enhanced but capability electron-accepting would be weakened with the number of wrapped corannulene increasing from one to two. The investigations on the charge transport properties of the complexes indicated the electron transport was more efficient and fast than the hole when C_{70} interacts with two corannulene molecules by its polar positions. In additional, the modification of C_{70} on its equatorial position with two corannulene is better for acquiring relative high charge mobility than on polar position with one or two. We hope that the present study would be helpful for the deep understanding to the effects of corannulene–fullerene noncovalent interactions on their behavior of charge transport and optical properties.

Acknowledgements

This project was funded by the National Natural Science Foundation of China (No. 21663024, 21362029 and 21663025), the China Postdoctoral Science Foundation (No. 2016M602809), and the Youth Science Research Funds of Tianshui Normal University (TSA1507).

References

1 V. Georgakilas, M. Otyepka, A. B. Bourlinos, V. Chandra, N. Kim, K. C. Kemp, P. Hobza, R. Zboril and K. S. Kim, *Chem. Rev.*, 2012, **112**, 6156–6214.
2 C. Romero-Nieto, R. Garcıa, M. A. Herranz, C. Ehli, M. Ruppert, A. Hirsch, D. M. Guldi and N. Martin, *J. Am. Chem. Soc.*, 2012, **134**, 9183–9192.
3 A. Bessette and G. S. Hanan, *Chem. Soc. Rev.*, 2014, **43**, 3342–3405.
4 J. Lohrman, C. Zhang, W. Zhang and S. Ren, *Chem. Commun.*, 2012, **48**, 8377–8379.
5 Z. Dai, L. Yan, S. M. Alam, J. Feng, P. R. D. Mariathomas, Y. Chen, C. M. Li, Q. Zhang, L.-J. Li, K. H. Lim and M. B. Chan-Park, *J. Phys. Chem. C*, 2010, **114**, 21035–21041.
6 B. W. Smith, M. Monthioux and D. E. Luzzi, *Nature*, 1998, **396**, 323–324.
7 M. Monthioux, *Carbon*, 2002, **40**, 1809–1823.
8 A. de Juan and E. M. Perez, *Nanoscale*, 2013, **5**, 7141–7148.
9 K. Yuan, Y. J. Guo and X. Zhao, *J. Phys. Chem. C*, 2015, **119**, 5168–5179.
10 K. Yuan, Y. J. Guo and X. Zhao, *Phys. Chem. Chem. Phys.*, 2014, **16**, 27053–27064.
11 K. Yuan, J. S. Dang, Y. J. Guo and X. Zhao, *J. Comput. Chem.*, 2015, **36**, 518–528.
12 K. Yuan, Y. J. Guo, T. Yang, J. S. Dang, P. Zhao, Q. Z. Li and X. Zhao, *J. Phys. Org. Chem.*, 2014, **27**, 772–782.
13 F. G. Klarner and T. Schrader, *Acc. Chem. Res.*, 2013, **46**, 967–978.
14 L. M. Salonen, M. Ellermann and F. Diederich, *Angew. Chem., Int. Ed.*, 2011, **50**, 4808–4842.
15 Y. Matsuo, K. Morita and E. Nakamura, *Chem.–Asian J.*, 2008, **3**, 1350–1357.
16 G. J. Bahun and A. Adronov, *J. Polym. Sci., Part A: Polym. Chem.*, 2010, **48**, 1016–1028.
17 C. Walgama, N. Means, N. F. Materer and S. Krishnan, *Phys. Chem. Chem. Phys.*, 2015, **17**, 4025–4028.
18 P. D. Tran, A. Le Goff, J. Heidkamp, B. Jousselme, N. Guillet, S. Palacin, H. Dau, M. Fontecave and V. Artero, *Angew. Chem., Int. Ed.*, 2011, **50**, 1371–1374.
19 A. Joshi and C. N. Ramachandran, *Phys. Chem. Chem. Phys.*, 2016, **18**, 14040–14045.
20 A. Cominetti, A. Pellegrino, L. Longo, A. Tacca, R. Po, C. Carbonera, M. Salvalaggio, M. Baldrighi and S. V. Meille, *Mater. Chem. Phys.*, 2015, **159**, 46–55.
21 M. I. Sluch, I. D. W. Samuel and M. C. Petty, *Chem. Phys. Lett.*, 1997, **280**, 315–320.
22 T. Gareis, O. Kothe and J. Daub, *Eur. J. Org. Chem.*, 1998, **8**, 1549–1557.
23 C. Carati, N. Gasparini, S. Righi, F. Tinti, V. Fattori, A. Savoini, A. Cominetti, R. Po, L. Bonoldi and N. Camaioni, *J. Phys. Chem. C*, 2016, **120**, 6909–6919.
24 A. V. Nikolaev, T. J. S. Dennis, K. Prassides and A. K. Soper, *Chem. Phys. Lett.*, 1994, **223**, 143–148.
25 G. Casella and G. Saielli, *New J. Chem.*, 2011, **35**, 1453–1459.
26 P. A. Denis and M. Yanney, *RSC Adv.*, 2016, **6**, 50978–50984.
27 D. Josa, I. Gonzalez-Veloso, J. Rodriguez-Otero and E. M. Cabaleiro-Lago, *Phys. Chem. Chem. Phys.*, 2015, **17**, 6233–6241.
28 D. Josa, L. A. dos Santos, I. Gonzalez-Veloso, J. Rodriguez-Otero, E. M. Cabaleiro-Lagoc and T. de Castro Ramalho, *RSC Adv.*, 2014, **4**, 29826–29833.
29 D. Josa, J. Rodriguez-Otero, E. M. Cabaleiro-Lago, L. A. Santos and T. C. Ramalho, *J. Phys. Chem. A*, 2014, **118**, 9521–9528.
30 S. Grimme, J. Antony, S. Ehrlich and H. Krieg, *J. Chem. Phys.*, 2010, **132**, 154104–154119.
31 L. Goerigk and S. Grimme, *Phys. Chem. Chem. Phys.*, 2011, **13**, 6670–6688.
32 Y. Zhao and D. G. Truhlar, *J. Am. Chem. Soc.*, 2007, **129**, 8440–8442.
33 T. M. Simeon, M. A. Ratner and G. C. Schatz, *J. Phys. Chem. A*, 2013, **117**, 7918–7927.
34 S. F. Boys and F. Bernardi, *Mol. Phys.*, 1970, **19**, 553–566.
35 R. A. Marcus, *Rev. Mod. Phys.*, 1993, **65**, 599–610.
36 H. Liu, S. Kang and J. Y. Lee, *J. Phys. Chem. B*, 2011, **115**, 5113–5120.
37 E. R. Johnson, S. Keinan, P. Mori-Sanchez, J. Contreras-Garcia, A. J. Cohen and W. Yang, *J. Am. Chem. Soc.*, 2010, **132**, 6498–6506.
38 T. Lu and F. Chen, *J. Comput. Chem.*, 2012, **33**, 580–592.
39 T. Lu and F. Chen, *J. Mol. Graphics Modell.*, 2012, **38**, 314–323.
40 M. J. Frisch, G. W. Trucks, H. B. Schlegel, G. E. Scuseria, M. A. Robb, J. R. Cheeseman, G. Scalmani, V. Barone, B. Mennucci, G. A. Petersson, H. Nakatsuji, M. Caricato, X. Li, H. P. Hratchian, A. F. Izmaylov, J. Bloino, G. Zheng, J. L. Sonnenberg, M. Hada, M. Ehara, K. Toyota, R. Fukuda, J. Hasegawa, M. Ishida, T. Nakajima, Y. Honda, O. Kitao, H. Nakai, T. Vreven, J. A. Montgomery Jr,

J. E. Peralta, F. Ogliaro, M. Bearpark, J. J. Heyd, E. Brothers, K. N. Kudin, V. N. Staroverov, R. Kobayashi, J. Normand, K. Raghavachari, A. Rendell, J. C. Burant, S. S. Iyengar, J. Tomasi, M. Cossi, N. Rega, J. M. Millam, M. Klene, J. E. Knox, J. B. Cross, V. Bakken, C. Adamo, J. Jaramillo, R. Gomperts, R. E. Stratmann, O. Yazyev, A. J. Austin, R. Cammi, C. Pomelli, J. W. Ochterski, R. L. Martin, K. Morokuma, V. G. Zakrzewski, G. A. Voth, P. Salvador, J. J. Dannenberg, S. Dapprich, A. D. Daniels, O. Farkas, J. B. Foresman, J. V. Ortiz, J. Cioslowski and D. J. Fox, *Gaussian 09, Revision D.01*, Gaussian, Inc., Wallingford CT, 2013.

41 L. Zoppi, J. S. Siegel and K. K. Baldridge, *Wiley Interdiscip. Rev.: Comput. Mol. Sci.*, 2013, **3**, 1–12.

42 K. K. Baldridge and J. S. Siegel, *Theor. Chem. Acc.*, 1997, **97**, 67–71.

43 T. Iwamoto, Y. Watanabe, T. Sadahiro, T. Haino and S. Yamago, *Angew. Chem., Int. Ed.*, 2011, **50**, 8342–8344.

44 T. Iwamoto, Y. Watanabe, H. Takaya, T. Haino, N. Yasuda and S. Yamago, *Chem.–Eur. J.*, 2013, **19**, 14061–14068.

45 T. Kawase and H. Kurata, *Chem. Rev.*, 2006, **106**, 5250–5273.

46 I. Garcia Cuesta, T. B. Pedersen, H. Koch and A. Sanchez de Meras, *ChemPhysChem*, 2006, **7**, 2503–2507.